Evaluation of the Effect of Boundary Layer Ingestion on the Performance of the Counter Rotating Turbo Fan CRISP by Means of Experimental Data

G. Charroin, T.Lengyel-Kampmann
DLR Institute of Propulsion Technology, Fan and Compressor Department
Linder Höhe, 51147 Köln, Germany
guillaume.charroin@dlr.de, timea.lengyel@dlr.de

Abstract

As global warming becoming an important concern, the aeronautic industry has to become environmental-friendlier. The innovation industry in propulsion system has developed new technologies which meets environmental targets such as decreasing noises, CO2 emissions and fuel consumption. Indeed, studies on aircraft engine components such as the Counter Rotating Turbo Fan (CRTF) or on the integration of an engine on airplanes such as the Boundary Layer Ingestion (BLI) are good examples of how researchers are trying to change this industry. The CRTF is a turbo fan with two rotors each rotating in opposite directions. A BLI enables the engine to ingest a part of the fuselage boundary layer and reaccelerate it by embedding the nacelles into the fuselage.

This paper shows the effect of the BLI on the CRISPmulti fan performance. In the frame of this project, a counter rotating fan was designed by DLR. A specification of this fan is that the blades are made of CFRP (Carbon Fiber Reinforced Plastic) with a thermoplast matrix, a composite material. It enables the blades to be lighter and to have a better acoustic and aerodynamic performance. This paper discusses about the analysis of data obtained during the experimental campaign conducted from February to June 2022 in the DLR test facility at Cologne. First, these experiments evaluate the aerodynamic performance with a clean inflow. Second, it determines the impact of a BLI, simulated by an inlet distortion system which creates a decrease of the total pressure within a part of the canal, upstream the fan.

As a consequence of these experiments, the effect of the distorted inflow is shown through two analysis. On the one hand, this study presents the evolution of different quantities when the inlet distortion system is going through the canal in radial direction. Therefore, it shows how the mass flow, total pressure ratio and engine power progress with different degrees of embedding. On the other hand, this study highlights the differences on the aerodynamic performance due to the inlet distortion. In this way it compares operating points with or without the inlet distortion through the performance map and the distribution of the total pressure and temperature on the outlet plane. These plots were generated by analyzing the measured data from the pressure and temperature rakes used during the circumferential traversing of the inlet distortion.

Keywords—Counter Rotating Fan, BLI, Experiments

I. INTRODUCTION

The main goal of the aircraft industry is to become more environmentally friendly especially by improving the performance of the engines, reducing the fuel consumption and flght emissions. In order to achieve this, the research is developing a lot of technologies such as counter-rotating fans and concept of BLI. DLR works since many years on several projects concerning these concepts. One of these projects named CRISPmulti is the continuation of the CRISP (Counter Rotating Integrated Shrouded Propfan) program carried out between 1985 and 2000 in collaboration with the MTU Aero Engines AG. The target of this program was to develop a concept of a turbofan engine using two rotors each rotating in opposite direction to increase the isentropic fan efficiency. However, the disadvantages due to the complexity of the mechanical system such as the weight stopped the program. In 2010, the advancements in composites materials and in calculation and optimization methods permit to relaunch the project. A new blade design by using CFRP as materials (Fig. 1) was optimized by a coupling of CFD and FEM simulations. The CRISPmulti project was thus carried out in order to validate the fan performances by using experimental means.

Fig. 1. CRISPmulti blade

Another research subject to achieve the aviation goals is the integration of engines in order to embed it in the fuselage and create boundary layer ingestion engine inflow conditions (Fig. 2). In this context, the CRISPmulti fan was selected to evaluate experimentally the effect of a BLI on its aerodynamical performances within the DLR's internal project AGATA.

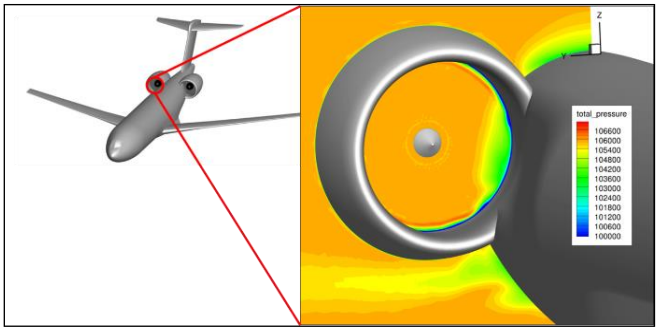

Fig. 2. Picture of embedded engine creating a BLI [3]

II. CRISPMULTI FAN

This section aims to provide an overview on the CRISPmulti fan. Therefore, the fan design process and a test setup and fan performance overview is shown.

A. Fan design

The CRISPmulti fan was designed to be used in a test rig in order to carry out experimental investigations. This is why, the optimization process was done under some constrains presented in the TABLE I. and targets of maximizing the efficiency and the stall margin. The fan was designed for one operating point called Aerodynamic Design Point (ADP). The optimization results are presented in the TABLE II. compared to the first version of the CRISP concept (CRISP1m) of the 1990's to highlight the improvements and differences.

After obtaining the final geometry of the blades, they were manufactured at the DLR Institute of Structures and Design in Stuttgart and then mounted on the test rig to launch the experimental campaign. (Fig. 3)

TABLE I. CONSTRAINS FOR THE OPTIMIZATION [2]

Design constrains		*Level*
Rig constrain	Blade number of Rotor1	10
	Blade number of Rotor2	12
	Hub-to-tip ratio	0,27
	Outer diameter (m)	1
Design goal	Tip clearence at R1 @ADP (mm)	0,65
	Tip clearence at R2 @ADP (mm)	0,5
	Exit swirl @ADP (°)	<3
	Axial Mach number	0,69

TABLE II. OPTIMIZATION RESULTS [2]

Optimisation result		*CRISP1m*	*CRISPmulti*
Design targets	Max. is.efficiency (%)	87	93
	Max. stall margin (%)	10	>10
Other free parameters	Speed ratio R2 to R1	0,86	0,79
	100% speed of R1 (RPM)	4980	5044
	Fan pressure ratio @ADP	1,25	1,30
	Mass flow @ADP (kg/s)	166	159

Fig. 3. CRISPmulti fan mounted on the test rig

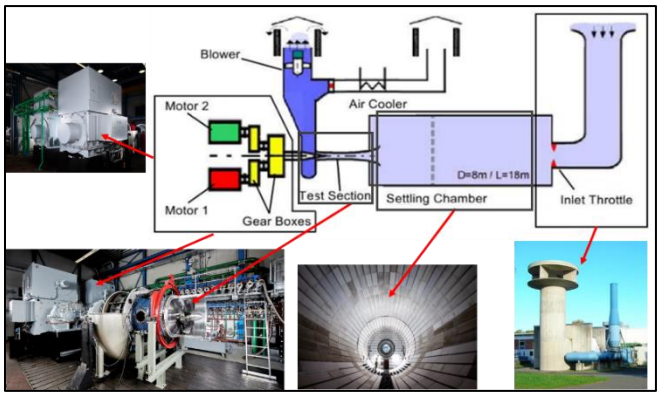

Fig. 4. M2VP test facility

B. Test setup and fan performance

The experimental investigation was carried out in the M2VP test facility (Fig. 4) at the DLR Institute of Propulsion Technology in Cologne. This facility allows the experimental investigations of fans and compressors. The air enters into an inlet tower and then through a 90° flow turning it arrives to a settling chamber. From this chamber the air is flowing into the inlet duct through the bellmouth. It allows a maximal diameter of 1m for the tested object and permits to reach a maximal massflow of 180 kg/s. A ring throttle is available to set the operating point of the tested machine. The flow arrives into the outflow duct behind the throttle and leave the channel through a silencer. The rotors of the tested object are driven by two electric motors (with a maximal power of 5MW for each one) through a gearbox system. This mechanical system enables the tested compressor to reach a maximal rotating speed of 20 000 RPM. A complex oil system is used to lubricate all rotating elements.

The first aim of these experiments was to check the optimization. For this purpose, many measuring devices have been used, but only those related to the aerodynamic performance are presented in this chapter. Indeed, in the first set up only the total pressure and the total temperature were evaluated. This is why, these quantities were measured with rakes at two locations in the test channel, at the plane E1 as inlet and at the plane E6 as outlet (Fig. 5).

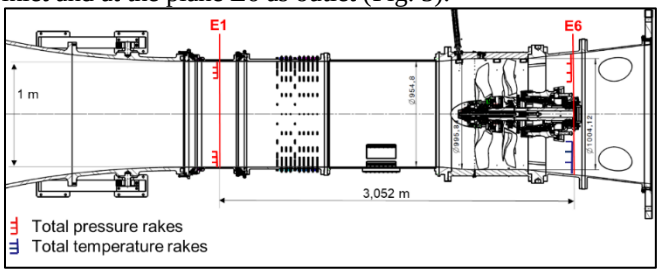

Fig. 5. Drawing of the test set up

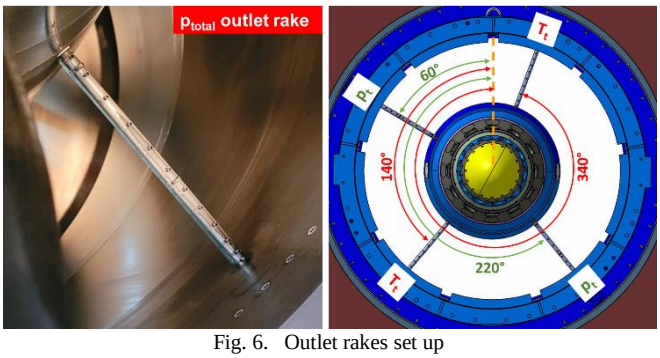

Fig. 6. Outlet rakes set up

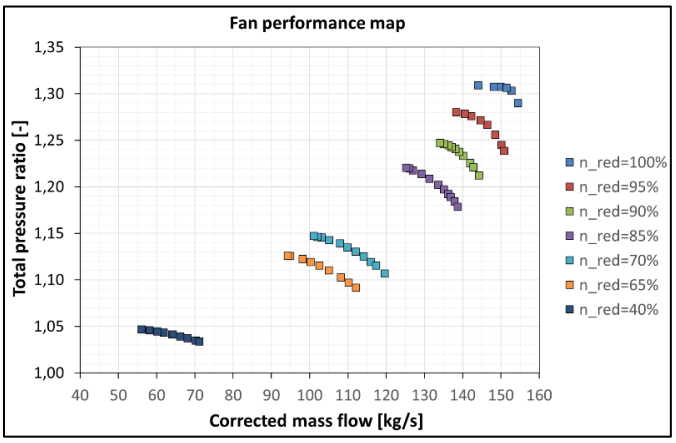

Fig. 7. Compression map of the CRISPmulti fan [1]

The rakes enable to have the radial distribution of the temperature and the pressure and based on this, the calculation of the total pressure ratio and the isentropic efficiency. Each rake is composed of 12 sensors. (Fig. 6)

In order to validate the aerodynamic performance of the CRISPmulti fan, these experimental data were analyzed. That permits to visualize the performance map. Indeed, the measurement of the total pressure permits to calculate the total pressure ratio π and have the compression map. The total temperature enables to calculate the isentropic efficiency which is very difficult to determine by this method for low pressure ratio fans due to the uncertainties. The study was therefore focused on the pressure.

The compression map is the plotting of the total pressure ratio π over the corrected massflow $\dot{m}_c$ defined as following equations:

$$\pi = \frac{P_{t,outlet}}{P_{t,inlet}} \quad (1)$$

$$\dot{m}_c = \dot{m} \frac{P_{ISA}}{P_{t,inlet}} \sqrt{\frac{T_{t,inlet}}{T_{ISA}}} \quad (2)$$

Where $T_{ISA} = 288{,}15$ K and $P_{ISA} = 101325$ Pa

This kind of map shows several speedlines which correspond to different rotational speeds which are a percentage of the nominal speed used during the design process. Thus, the Fig. 7 highlights the compression characteristics of the CRISPmulti fan.

III. Inlet Distortion Effect

The second aim of the experimental campaign concerns the AGATA project. Indeed, as explained before, this project was carried to show the effect of a BLI on the performance of the CRISPmulti fan. Some effects are highlighted through this study which will be presented in three parts. The first one is a presentation of the inlet distortion device representing the BLI. The second one is an analysis of the evolution of quantities like mass flow, total pressure ratio and the engine power during the using of the device. The last one is a comparison between with and without distortion.

A. Test setup with an inlet distortion

The test bed changed during the measurement with the distortion. A part of the channel upstream the fan is modified where a distortion device and a honeycomb are added, as presented in theFig. 8. The inlet distortion is thus created by a

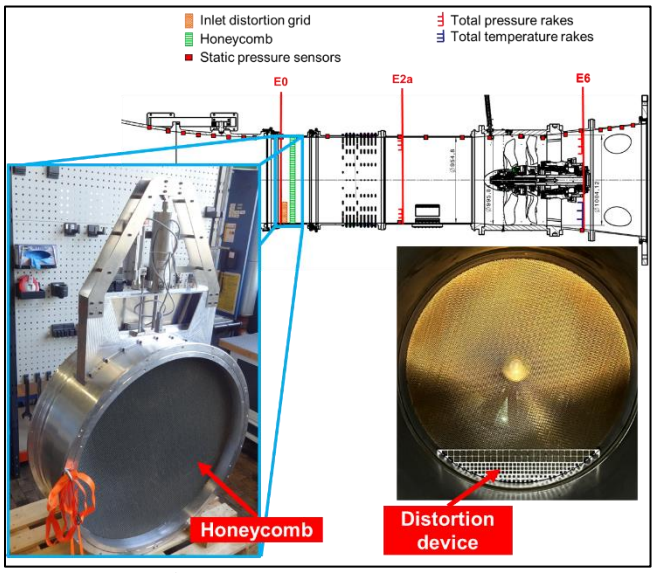

Fig. 8. Drawing of the test bed with some instrumentations and distortion devices

grid traversing the inlet channel in the radial direction. Downstream this device, there is a honeycomb which allows to have a more homogenous inflow. In this test setup showed in the Fig. 8, the inlet total pressure is measured at the plane E2a and the outlet total pressure and total temperature are still measured at the plane E6.

The measurement of total pressure at the inlet plane enables to check if the distortion has a comparable behavior with a BLI. The Fig. 9 shows a decreasing of the total pressure in the area of the distortion as happened with a BLI.

The advantage of this device is that the distortion grid can have two degrees-of-freedom. Indeed, there is a circumferential rotation around the axis X. This enables to measure the distribution on an entire plane of the total temperature and the total pressure like in Fig. 9. These quantities are measured thanks to a rake which cannot move and is a line of sensor in the radial direction at different radius. As it is impossible to move the rakes, the distortion device rotates in all circumferential positions to be able to measure the quantities for different angles and so for the entire plane.

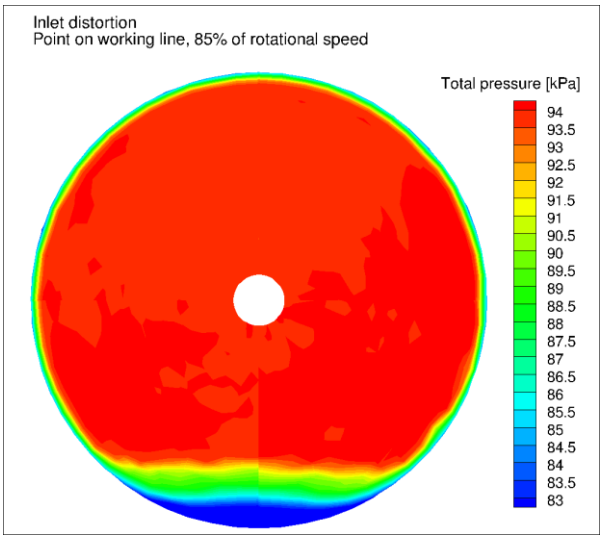

Fig. 9. Inlet total pressure distribution

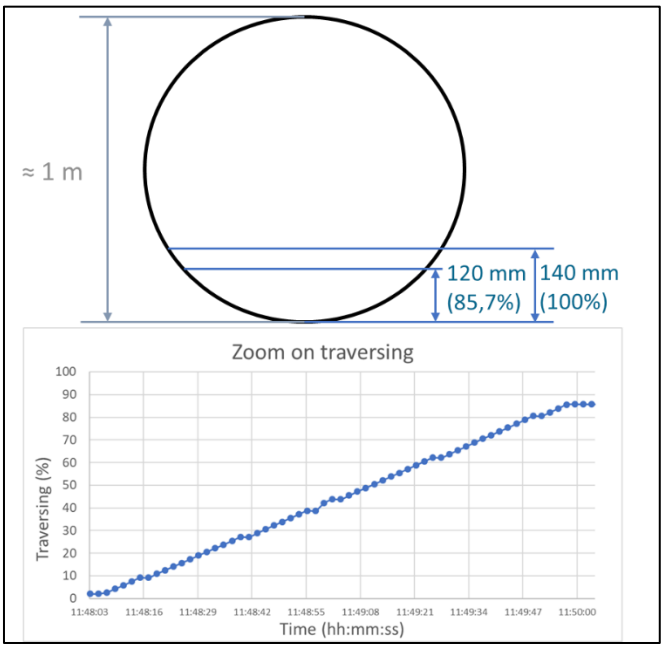

Fig. 10. Variation the immersion depth

Moreover, one translation is possible in the radial direction through the channel. This movement permits to change the immersion depth of the grid and therefore to model the BLI with different degree of embedding. The grid goes through the whole channel until 140 mm but in this study the maximal immersion depth is 120 mm (85,7% of its capacity), as presented in the Fig. 10. This height represents around 15% of the whole channel which is a small distortion.

B. Evaluation of BLI effect

1) Evolution of quantities during the grid traversing in the radial direction

The previously presented process permits to analyze the evolution of different quantities during the traversing of the grid. This part shows the effect of a BLI with different degrees of distortion from 0 mm (0%) to 120 mm (85,7%) of immersion depth as showed in the graph of the Fig. 10. The graphs in the Fig. 11 present the results for the corrected massflow, the total pressure ratio and the calculated power of both rotors. This analysis considers the experimental data for one operating point with a speed of 85% of the nominal speed and in the stall area. Firstly, for the massflow, the graph shows that it is still almost constant around 125 kg/s for the different immersion depth. Therefore, the inlet distortion has a minor effect on the mass flow. Then for the total pressure ratio which is plotted in relative value on the maximum 1,2015. The distortion has an effect because even if the decreasing is not so important until 40% of the immersion depth, after the whole traversing the total pressure decreases by 1,5%. This behavior is also visible for the calculated motor power, also plotted as relative value on the maximum (990500 W for the rotor 2 and 1092502 W for the rotor 1). This power is calculated by multiplying the speed of the motor with the moment of the motor. So, the power is not the direct power of the rotor but the powers of the motor and the losses between motor and rotor with the gearbox are not considered. Indeed, the power of the motor was measured by

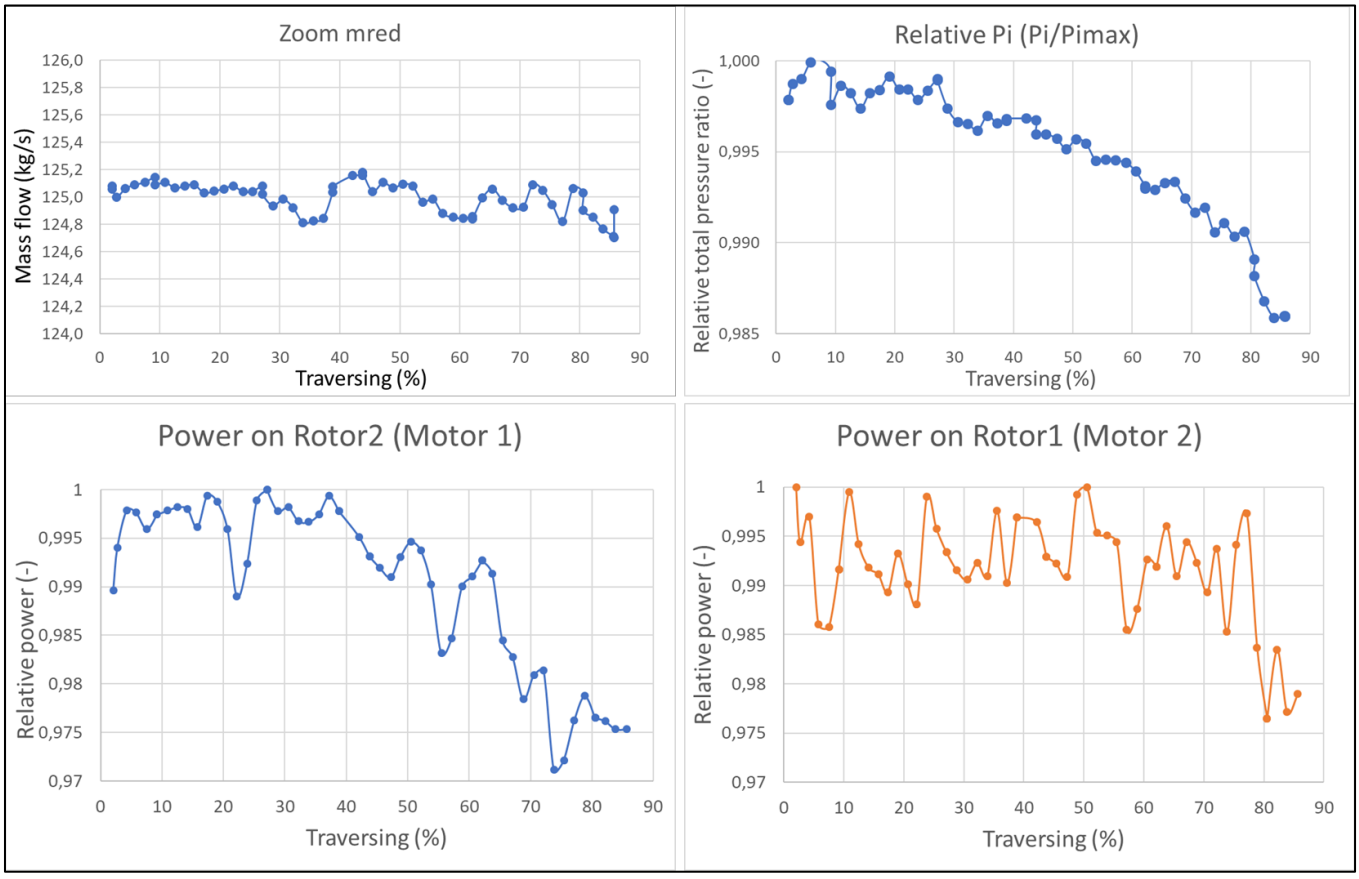

Fig. 11. Evolution of the corrected mass flow, total pressure and power of both rotors during the traversing

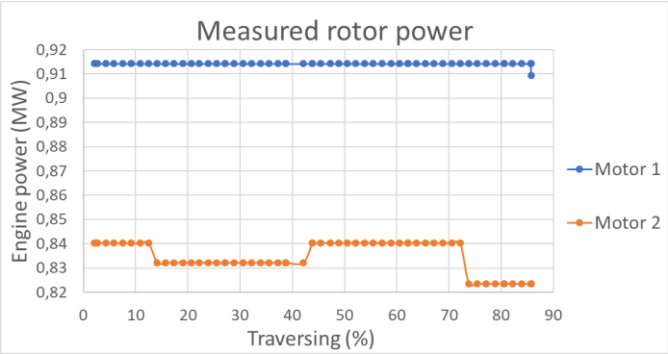

Fig. 12. Measured rotor power with the function process

following a function which does not allow to save the data continuously but only when the change is too important.

This measured rotor power like in the Fig. 12 is not usable because it shows some steps of change but not the exact value for each measurement. Finally, it was decided to use the calculated motor power to have an idea on the effect of the BLI on the power. Moreover, in the test setup, the motor 1 drives the rotor 2 and the motor 2 drives the rotor 1. In this analysis, the both motor powers decreased of 2,5% during the traversing. This highlights an effect of the BLI on the airplane engine also presented by A. Vinz [5] which is a decreasing of the power.

2) BLI effect through a comparison with and without distortion

The second part of the study is a comparison between with and without inlet distortion which shows some effects of the BLI. This following analysis was done for five different experimental operating points with three different speeds (95%, 85%, 65% of the nominal speed) in black in the Fig. 13. Three of these points are on the working line and two others on the stall area of the speedlines 65% and 85%. In this part, the immersion depth of the distortion grid is 120 mm except for the point at 95% of speed for which it was measured with a depth of 70 mm. In this chapter, only the results of some points are presented.

The Fig. 14 presents the experimental outlet distribution of the total pressure in top part and the total temperature at the bottom. That is a comparison between without distortion at the left and with distortion at the right for the operating point on the working line with a speed of 85% of the nominal speed. The quantities are plotted in relative value by dividing the maximum for the both cases (with and without distortion). The maximal value for the total pressure is 113 kPa and for the total temperature 317 K.

For this point in Fig. 14, the distortion decreases the total pressure on the outlet plane by about 0,5% where there is no distortion and until 2% in the inlet distortion area boxed on the second picture. As for the total temperature, it increases also and especially where there is the distortion grid.

In the Fig. 15, the effect of the distortion with different speeds is highlighted. Indeed, the operating point with 85% of nominal speed (in red at right) is compared with another operating point on the working line but with a speed of 65% (in blue at left). The relative value is calculated with the same maximum as previously for the 85% but for the 65% its own maximum is used, that is 106 kPa for the total pressure and

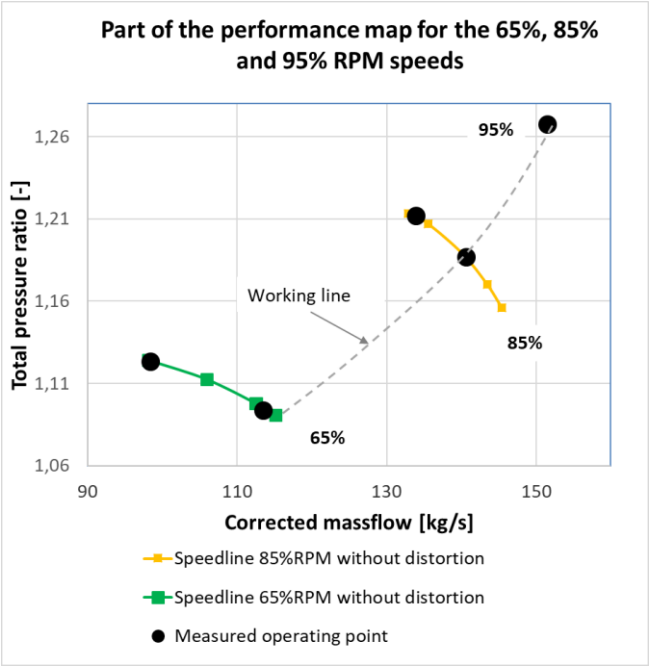

Fig. 13. Part of the performance map highlighting the measured operating point analyzed in this study

309 K for the total temperature. That permits to see an equivalent variation of quantities.

Therefore, this figure shows that the total pressure and the total temperature change less for the 65% of speed than for the 85%. The decrease of total pressure is of 0,5% for the lowest speed and the increase of total temperature is of about 1% against 2% for the pressure and 1,5% for the temperature with the highest speed. In conclusion, the higher the speed, the greater the effect of the distortion.

This analysis can be done also on the other operating points and the TABLE III. summarizes the comparison for the five points with a percentage of decreasing in blue and increasing in red in comparison of without distortion. The same observations can be done as in previous results by calculating the area averaged values for each plane. The total pressure ratio decreases with the distortion and more for the higher rotational speeds than the lower ones. The total temperature increases with the distortion and the difference between the different speeds is less important. But it is not easy to conclude quantitatively on the total temperature because of the errors on the measurement. For the engine power, globally it decreases and especially the motor 1 which drive the second rotor.

The results for the operating point with a speed of 95% are different because the immersion depth of the inlet distortion is way lower than for other points. So, it has a slight effect on the result.

TABLE III. SUMMARY OF COMPARISON BETWEEN WITH AND WITHOUT DISTORTION

Operating Point	Total pressure ratio	Total temperature	Power	
			Motor 1	Motor 2
95% RPM	0,07% ↘	0,14% ↗	0,93% ↗	0,66% ↗
85% RPM Working-line	0,47% ↘	0,28% ↗	2,93% ↘	0,34% ↘
85% RPM Stall Area	0,27% ↘	0,34% ↗	1,76% ↘	0,46% ↘
65% RPM Working-line	0,04% ↘	0,41% ↗	1,02% ↘	0,54% ↗
65% RPM Stall Area	0,09% ↘	0,36% ↗	0,61% ↘	0,23% ↘

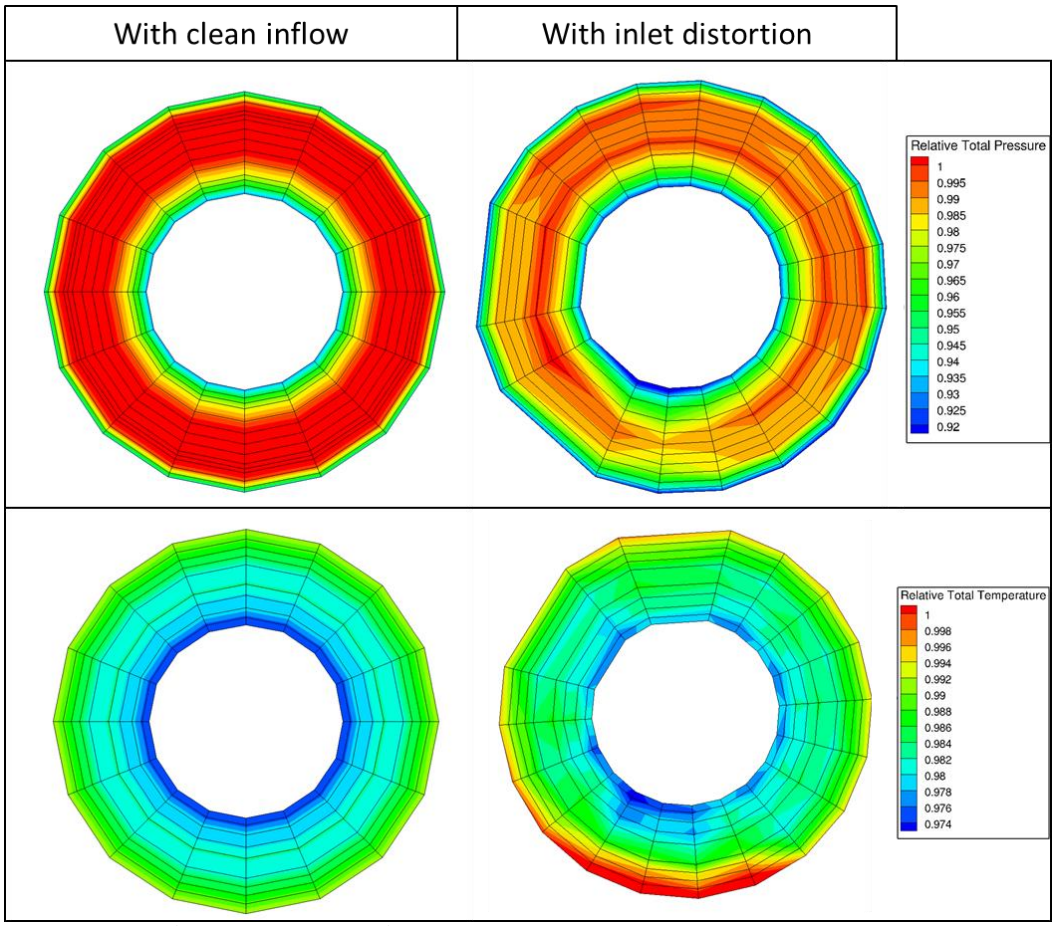

Fig. 14. Comparison of the outlet distribution of total pressure and temperature between with and without distortion (85% RPM)

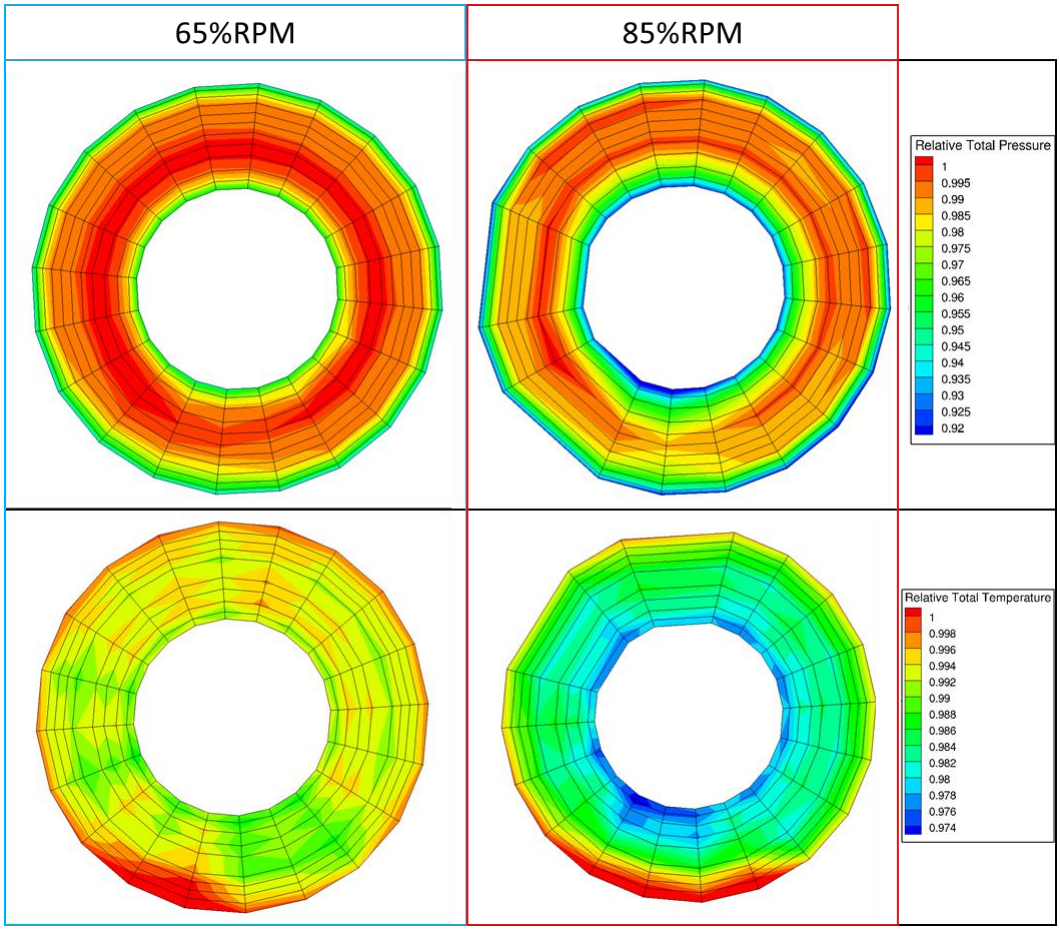

Fig. 15. Effect of the inlet distortion for two different speeds

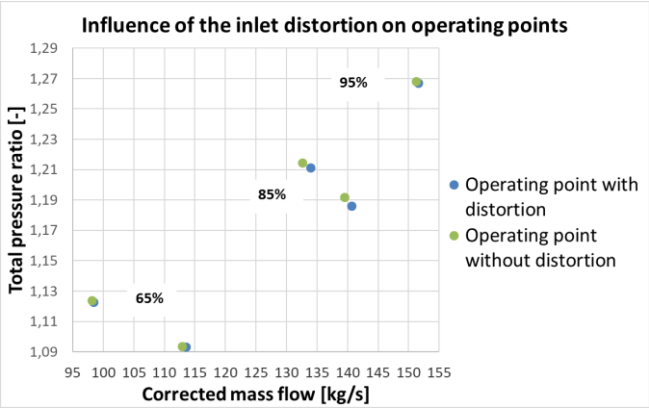

Fig. 16. Final effect of the distortion om the performance map

The Fig. 16 concludes the effect of the distortion on the performance map. The differences between with and without distortion are not high because the distortion is small. But for all points the same trend is visible which is a decreasing of the total pressure ratio again and an increasing of the corrected mass flow. This trend is similar to the CFD results presented in the paper of V. Jerez Fidalgo [6]. The effect of the distortion is again lower for the speed of 65%.

The last point concerning the effect of the distortion is the distribution of the static pressure along the casing. For this analysis, the static pressure is measured behind the distortion for the case with distortion and when the distortion is in an opposite circumferential position to have a clean inflow for the case without distortion. Therefore, the measuring points presented in the Fig. 17 have been used to create the Fig. 18. The Fig. 18 shows the relative variation of the static pressure ΔP defined with the following equation:

$$\Delta P = \frac{P_{S,undistorted} - P_{S,distorted}}{P_{T,inlet,undistorted} - P_{T,inlet,distorted}} \quad (3)$$

This permits to compare the static pressure with distortion and without by normalizing this variation of static pressure with the variation of total pressure measured at the inlet (plane E2a).

For this operating point, $P_{T,inlet,undistorted} = 87{,}14\ kPa$ and $P_{T,inlet,distorted} = 82{,}52\ kPa$.

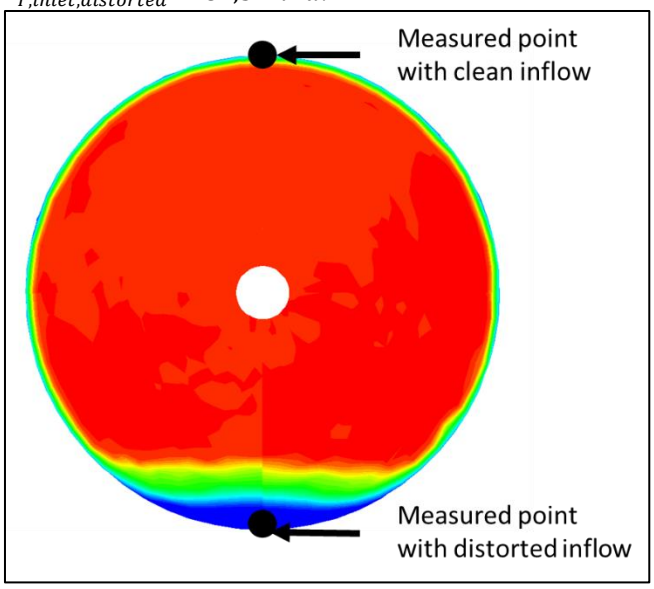

Fig. 17. Circumferential positions of point measuring static pressure

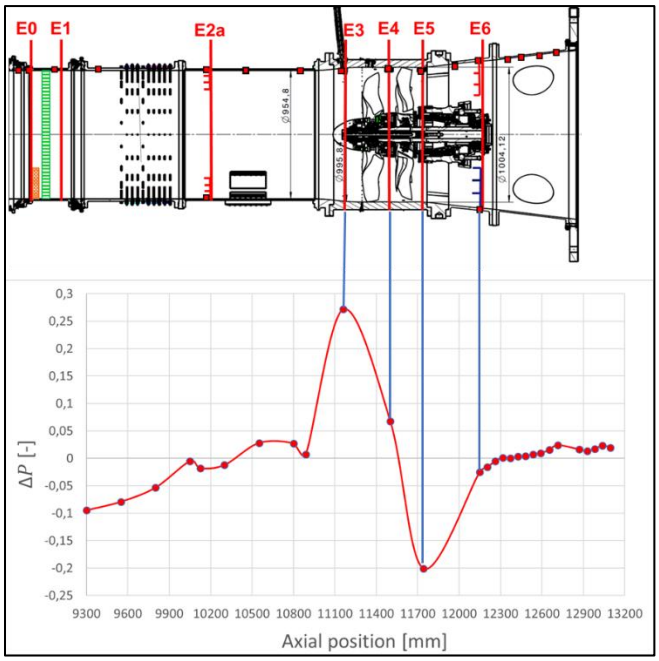

Fig. 18. Distribution of the relative static pressure variation along the casing

The graph in Fig. 18 shows that upstream the fan the static pressure is almost the same for the both configurations. But in front of the first rotor, the static pressure without distortion becomes more and more higher than behind the grid distortion. This can be explained by the acceleration of the flow with distortion which decreases the static pressure in comparison with a clean inflow. Then the opposite behaviour happens behind the second row. And the static pressure becomes again same for both cases downstream the fan. Even if the comparison could be improved with more points of measurement, this behaviour is comparable with the results in the literature written by Longley [7].

IV. Conclusion

In conclusion, this paper presented the CRISPmulti fan aerodynamic performance thanks to experimental data to be able to understand some effect of a BLI on this kind of concept. It explained also how was modeled the BLI in the test setup and what analysis of the experimental data is done to show this effect. The BLI changes the fan performance by shifting the operating point in the performance map with a decrease of the total pressure ratio. For the outlet total temperature, it increases with an inlet distortion. The differences concern the whole domain but especially the area downstream the distortion. Moreover, the effect of the BLI is higher with a high rotational speed. To finish, an important effect is also the decreasing of the engine power.

References

[1] G. Charroin, “Validation of the CFD simulation of a contrarotating fan with experimental data”, Master Thesis at INSA Hauts-de-France, France, September 2022.

[2] T. Lengyel-Kampmann, J. Karboujian, G.Charroin, P.Winkelmann, “Experimental Investigation Of An Efficient And Lightweight Designed Counter-Rotating Shrouded Fan Stage”, ETC2023 at Budapest, Hungary, April 2023.

[3] T. Lengyel-Kampmann, J. Karboujian, K. Koc, R. Schnell, P. Winkelmann, “Experimental Investigation On A Lightweight, Efficient, Counter-Rotating Fan With And Without Boundary Layer Ingestion”, CEAS Journal 2023.

[4] T. Lengyel-Kampmann, J. Karboujian, K. Koc, R. Schnell, P. Winkelmann, “Experimentelle Untersuchung An Einem In Leichtbauweise Ausgelegten, Effizienten, Gegenläufigen Fan Mit Und Ohne Grenzschichteinsaugung“, DLRK Konferenz at Dresden, 2022.

[5] A. Vinz, A. Raichle, “Investigation Of The Effects Of BLI Engine Integration On Aircraft Thrust Requirement”, DLRK Konferenz at Dresden, 2022.

[6] V. Jerez Fidalgo, C. A. Hall, Y. Colin, “A Study Of Fan-Distortion Interaction Within The Nasa Rotor 67 Transonic Stage”, ASME, Glasgow, UK, 2010

[7] J.P. Longley and E.M. Greitzer, “Inlet Distortion Effects In Aircraft Propulsion System Integration”, Cambridge University, England, 1992